Neutron Scattering Study on Dynamics of Water Molecules in MCM-41

Shuichi Takahara, Masatsugu Nakano, and Shigeharu Kittaka*

Department of Chemistry, Faculty of Science, Okayama University of Science, 1-1 Ridaicho, Okayama 700-0005, Japan

Yasushige Kuroda, Toshinori Mori, and Hideaki Hamano

Department of Chemistry, Faculty of Science, Okayama University, Tsushima, Okayama 700-8530, Japan

Toshio Yamaguchi

Department of Chemistry, Faculty of Science, Fukuoka University, Nanakuma, Jyonan-ku, Fukuoka 814-0180, Japan

Received: October 23, 1998; In Final Form: April 2, 1999

The dynamics of water molecules confined in MCM-41 was investigated by quasi-elastic neutron scattering. The measurement was performed for three water-filled MCM-41 samples with different pore sizes in the temperature range 200−300 K. The spectra were analyzed by using a model employed by Teixeria et al. in a study for bulk water. This model is composed of two motions of water molecules: rotational and translational diffusions. For the translational diffusion, water molecules in MCM-41 are, on the whole, less mobile than those in bulk water, and the mobility is decreased by narrowing of the pore size. The residence time of translational diffusion of the confined water molecules shows the Arrhenius type of temperature dependence, which is in contrast to a non-Arrhenius behavior for bulk water. This implies that a growth of the hydrogen-bond network of water is hindered in a confined space by surface field. Spectra of MCM-41 sample having monolayer water were also measured and could be analyzed with a model in which only rotational diffusion is an allowed motion of the monolayer water molecules.

Introduction

Liquid water is characterized by formation of a hydrogen-bond network which brings in many anomalous properties such as density maximum at 4 °C, singularity at −45 °C, etc.[1] It is interesting to study the mechanisms of how the structure and dynamics of the hydrogen-bond network are modified in a confined geometry. From the viewpoints of material science and biology, etc., it is important to study the physicochemical properties of this type of water to understand their roles in each field. Water molecules confined in nanospace such as porous silica have widely been investigated along this line,[2−4] but distributions of pore sizes often introduced ambiguity in interpretations of the experimental results. Families of siliceous MCM-41, which were developed by Beck et al. in 1992,[5] are one of the most suitable model samples, because they contain highly controlled cylindrical channels with very narrow pore size distribution. In due course, water molecules confined in MCM-41 have recently become an important target to investigate.[6−8]

In the present study, we have investigated the dynamics of water molecules confined in MCM-41 by neutron scattering in the temperature range 200−300 K. The first purpose of this study is to compare their dynamics with that of bulk water. The second one is to investigate dependence of their dynamics on pore size. MCM-41 samples with different pore sizes can be readily synthesized by varying template molecules. In addition, the dynamics of monolayer water molecules has been studied.

* Author for correspondence. E-mail: kittaka@chem.ous.ac.jp.

Experimental Section

Preparation of MCM-41 Samples. Three kinds of siliceous MCM-41 samples (C10, C14 and C18) were prepared by the method of Beck et al.[5] using alkyltrimethylammonium bromide with alkyl chains of 10, 14, and 18 carbon atoms, respectively. The MCM-41 samples were characterized by electron microscopy, X-ray diffraction, and N_2 adsorption measurements. The specific surface area and the pore radius calculated from the N_2 adsorption isotherms are listed in Table 1. Contents of sodium were determined by atomic absorption spectrometry and are also listed in Table 1.

Adsorption of Water. Adsorption isotherms of water were measured gravimetrically by using a Cahn 2000 electrobalance connected with a gas dosing system composed of a Baratron 390H pressure gauge. The temperature range of the measurement was 283−303 K. Before the measurement, the samples were evacuated at room temperature for about 12 h by using a turbomolecular pump. The waiting times for equilibration after dosing the water vapor were about 2 h in the region where the capillary condensation proceeds and 30 min in the other regions. The absolute amount of water adsorbed on each sample was determined as a sum of water content remaining after evacuation at room temperature and the adsorbed amount measured. The former value was determined by heating of the sample at 800 °C under vacuum.

DSC Measurements. Melting behaviors of water in the MCM-41 samples were checked by DSC (ULVAC DSC-7000) measurements. The measurements were performed for three water-filled samples (C10, C14, and C18) at a heating rate of

10.1021/jp984136j CCC: $18.00
Published on Web 06/30/1999

TABLE 1: Parameters Characterizing Each MCM-41 Sample

sample	sp. surf. area /$m^2 \cdot g^{-1}$	pore radius /nm	Na content /ppm	melting temp/K
C10	1096	1.07	180	
C14	1300	1.42	160	221
C18	837	1.87	100	242

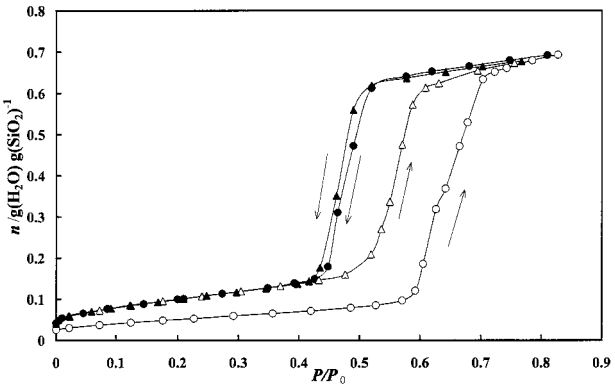

Figure 1. Adsorption isotherms of water for the C14 sample at 298 K. First and second runs are represented by circles and triangles, respectively. Adsorption and desorption branchs are represented by open and closed symbols, respectively.

5 K min^{-1} after cooling to 130 K. The water-filled samples were prepared by the same method as in the neutron scattering measurements described below.

Neutron Scattering. The neutron scattering measurements were carried out with a time-of-flight type spectrometer AGNES[9] installed at the JRR-3M reactor of Japan Atomic Energy Research Institute. The wavelength of the neutron beam was 4.22 Å, the momentum transfer range 0.61−2.38 $Å^{-1}$, and the measuring temperature range 200−300 K. A resolution function of the instrument was determined with a vanadium rod as a function of momentum transfer Q and energy transfer ω. The half-width at half-maximum of the resolution function was ca. 80 μeV. For the neutron scattering measurements, three kinds of water-filled MCM-41 samples (C10, C14, and C18) were prepared by the following procedures: the MCM-41 samples were evacuated for 12 h by using a turbomolecular pump at room temperature and then exposed to water vapor (relative pressure $P/P_0 = 0.7-0.8$) for 2 days at 298 K to achieve capillary condensation of water. The behavior of monolayer water on the MCM-41 pore surface was studied with the C18 sample which was prepared as follows. First, water-filled C18 sample was prepared in the same way as described above. Second, the water-filled sample was evacuated for 1 day by using a turbomolecular pump. Finally, the sample was exposed to water vapor ($P/P_0 = 0.4$) for 6 h. The first procedure should be performed so that the sample surface is fully hydroxylated.

Results and Discussion

Adsorption of Water. Figure 1 shows the adsorption isotherms of water for the C14 sample at 298 K. In the first adsorption (○), a sharp increase of water content due to the capillary condensation appears at $P/P_0 = 0.6-0.7$. Evidently, the desorption branch (●) does not run on the adsorption branch after reaching the topmost adsorption, and the condensed water is not desorbed until pressure is decreased down to $P/P_0 = 0.4-0.5$. Moreover, the desorption branch does not run on the adsorption branch in the monolayer adsorption region and does not come back to the origin of the first adsorption. The second adsorption (△) runs on the desorption branch of the first adsorption cycle, and the capillary condensation occurs at the pressure range $P/P_0 = 0.5-0.6$, lower than that in the first adsorption. The desorption branch of the second run (▲) is similar to that of the first run. Further repeated adsorption experiments gave similar curves for the second run. Similar results were obtained for the C10 and C18 samples. This kind of irreversibility is common to dried silica samples, and has been explained by the fact that the rate of hydroxylation of silica surface is slower than that of other metal oxide surfaces. Molar ratios of protons contained in surface hydroxyls, monolayer water, and capillary-condensed water were calculated for each sample by using adsorption isotherms, and are listed in Table 2. In this calculation, it was assumed that the amount of adsorbed water remaining under vacuum at room temperature is due to surface hydroxyls. The monolayer capacity estimated with the BET theory was used as the amount of monolayer water. These values were used in the analysis of neutron scattering spectra.

TABLE 2: Molar Fraction of Each Component of Adsorbed Water

sample	surface hydroxyls	monolayer water	capillary-condensed water
C10	0.043	0.168	0.789
C14	0.025	0.101	0.874
C18	0.018	0.075	0.907

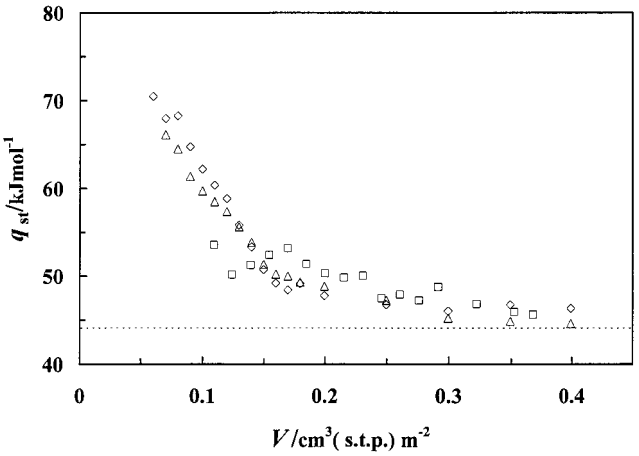

Figure 2. Isosteric heat of adsorption of water for C10 (◇), C14 (△), and C18 (□) samples as a function of adsorbed amount of water. A dotted line denotes the heat of liquefaction of bulk water at 298 K.

To assess the surface properties of the samples, the isosteric heat of adsorption of water (q_{st}) was calculated from the temperature dependence of the adsorption isotherms by using the Clausius−Clapeyron equation. Figure 2 shows q_{st} as a function of amount of adsorbed water. As shown in this figure, the result of the three samples are almost the same. This implies that interactions of surface hydroxyls with adsorbed water molecules are similar in the monolayer range on the three samples. Then, differences of dynamical properties of the water molecules confined in the present samples may singly be ascribed to the pore size effect.

DSC Measurements. Figure 3 shows the DSC curves of the water-filled samples. A broad endothermic peak due to melting of the confined water was observed on the C14 and C18 samples, while no peak was observed on the C10 sample. The peak temperatures are listed in Table 1. The melting temperature for the C14 and C18 samples decreases with pore size, obeying apparently the Gibbs−Thomson equation.[10] When the Gibbs−Thomson equation is applied to C10 sample, the deduced melting temperature is 193 K. However, the water in the C10 sample did not freeze down to 173 K. Similar phenomena have

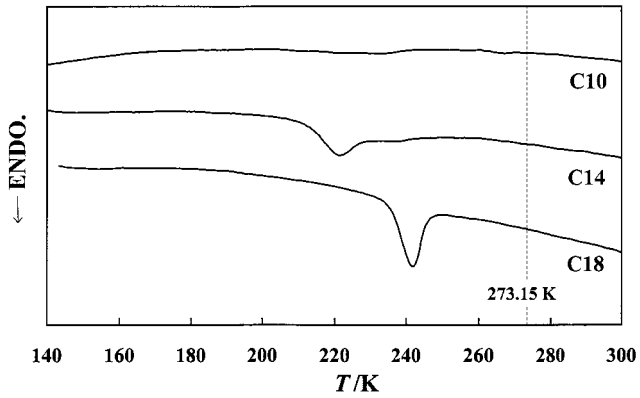

Figure 3. DSC curves for the water-filled MCM-41 samples determined at the heating rate 5 K min^{-1} after cooling to 130 K.

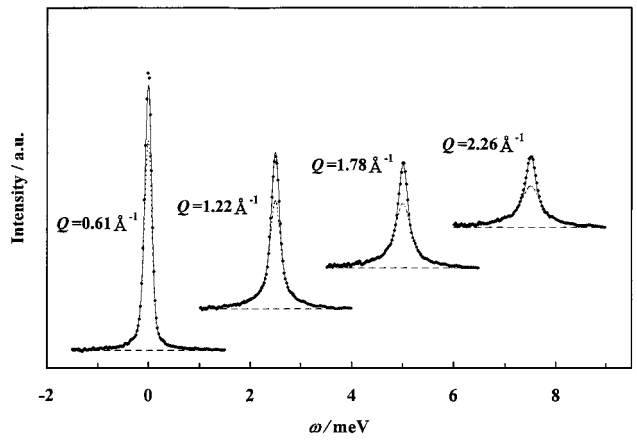

Figure 4. *Q*-dependence of neutron scattering spectra for the water-filled C10 sample at 300 K. Closed circles indicate the experimental data. Solid, dotted, and broken lines are for the total fit, the quasi-elastic component, and the background, respectively.

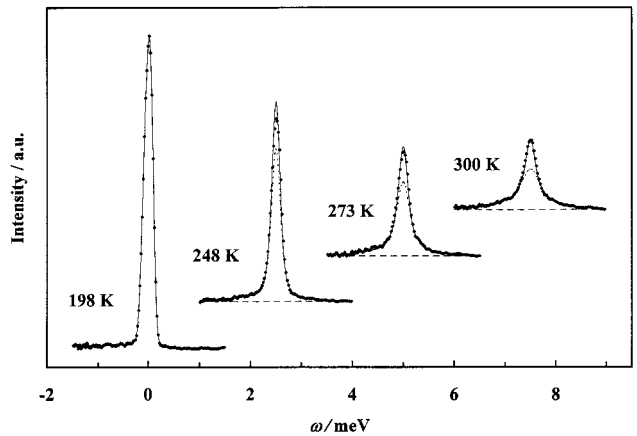

Figure 5. Temperature dependence of neutron scattering spectra for the water-filled C10 sample at $Q = 2.26$ $Å^{-1}$. Closed circles indicate the experimental data. Solid, dotted, and broken lines are for the total fit, the quasi-elastic component, and the background, respectively.

been found by XRD measurement.[8] It is interesting to detail the structure of nonfreezing water in the pore.

Quasi-elastic Neutron Scattering. *Results.* Typical examples of the quasi-elastic neutron scattering spectra are shown in Figures 4−7. Figure 4 shows the *Q*-dependence of the spectrum for the water-filled C10 sample at 300 K. Broadening of the peak with increase in *Q* values was observed. Figure 5 shows the temperature dependence of the spectrum for the water-filled C10 sample at $Q = 2.26$ $Å^{-1}$. The lower the temperature, the narrower the line width, indicating slowing of the motion of

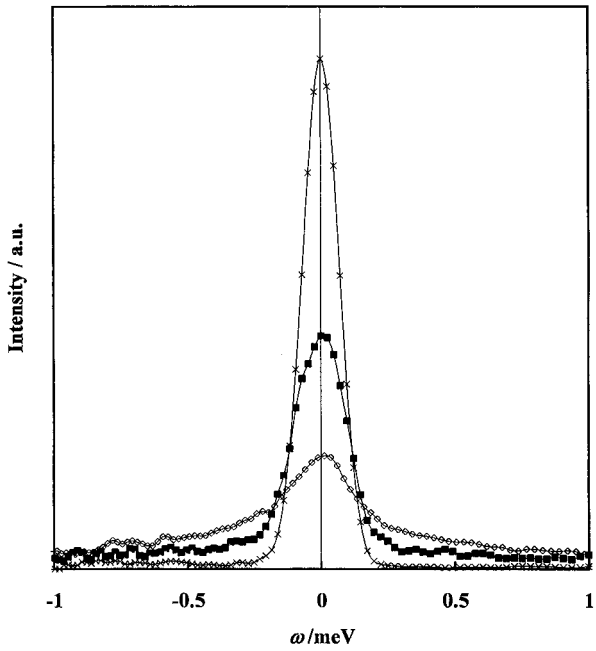

Figure 6. Neutron scattering spectra for the C18 sample having monolayer water (■), the water-filled C18 sample (◇), and vanadium (×), which were determined at 300 K and $Q = 2.26$ $Å^{-1}$.

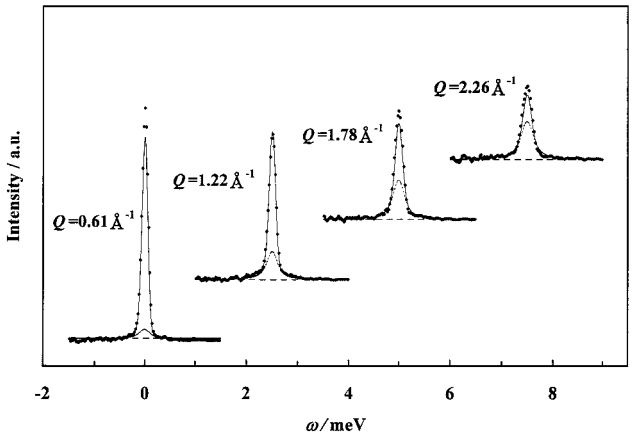

Figure 7. *Q*-dependence of neutron scattering spectra for the C18 sample having monolayer water at 300 K. Closed circles indicate experimental data. Solid, dotted, and broken lines are for the total fit, the quasi-elastic component, and the background, respectively.

the water molecules. The spectrum of the C18 sample having monolayer water determined at 300 K and $Q = 2.26$ $Å^{-1}$ is shown in Figure 6, together with the spectra of the water-filled C18 sample and vanadium (the resolution function of the instrument). Quasi-elastic scattering was clearly observed in the C18 sample having monolayer water, although a line width is narrower than that of the water-filled sample. This implies that the water molecules in the monolayer are mobile on the experimental time scale but less than those in the water-filled sample. Figure 7 shows the *Q*-dependence of the spectrum for the C18 sample having monolayer water at 300 K.

Data Analysis for Water-Filled Samples (Model 1). In the present study, the atoms other than protons in the samples virtually do not contribute to the spectra because of the extremely large incoherent scattering cross section of proton. Moreover, coherent scattering from O and Si was not actually counted because the main Bragg peaks of MCM-41 must appear in a lower *Q*-range than the measured ones. In the present analysis, we considered the motions of protons in the surface

TABLE 3: Parameters Obtained by Analysis of Neutron Scattering Spectra

sample	T/K	A	$D_T/10^{-10}$m^2 s^{-1}	L/Å	τ_T/ps	ΔE_T/kJ mol^{-1}	τ_R/ps	ΔE_R/kJ mol^{-1}
	300		14	0.76	4.1		2.5	
C10[a]	273	0.151	9.7	0.95	9.4	26	4.0	13
	248				35		7.6	
C14[a]	300	0.122	16	0.70	3.1	29	2.0	16
	241				52		9.2	
	300		17	0.67	2.6		1.6	
	273		7.7	0.71	6.6	24	3.0	
C18[a]	255	0.108			15		6.5	18
	241				80		8.6	
C18[b]	301	0.157					2.5	3.7
	273						3.0	
bulk[c]	298		23.0	0.50	1.10		1.10	7.74

[a] The results of the water-filled samples for model 1. [b] The results of the sample having monolayer water. [c] The literature values of bulk water in ref 12.

hydroxyls and the adsorbed water molecules. The mobility of water molecules neighboring the pore wall (monolayer water molecules) must be different from that of other water molecules (capillary-condensed water molecules). Then, the scattering law $S(Q,\omega)$ of the water-filled samples can be written as follows:

$$S(Q,\omega) = \exp(-Q^2\langle u^2\rangle/3)[A_1\delta(\omega) + A_2 S_{ml}(Q,\omega) + (1 - A_1 - A_2)S_{cc}(Q,\omega)] + B \quad (1)$$

Here, the first factor represents a Debye−Waller factor. $\delta(\omega)$ is a δ-function. $S_{ml}(Q,\omega)$ and $S_{cc}(Q,\omega)$ represent scattering laws of monolayer water and capillary-condensed one, respectively. A_1 and A_2 are the fraction of each component. B is for the ω-independent background due to vibrational motions. In eq 1, $A\delta(\omega)$ corresponds to an elastic component and is due to surface hydroxyls. Strictly speaking, elastic component is generated also when mobile atoms are confined in a narrow space.[2,11] However, this contribution is negligible in the present systems because the pore radius (10.7 Å for C10) is much larger than the inverse of momentum transfer (0.4−1.6 Å) corresponding to the measurable length scale. For $S_{cc}(Q,\omega)$, it is appropriate to use a model developed by Teixeria et al.[12] for bulk water, i.e.,

$$S_{cc}(Q,\omega) = S_R(Q,\omega) \otimes S_T(Q,\omega) \quad (2)$$

where $\otimes$ means a convolution in ω. $S_R(Q,\omega)$ and $S_T(Q,\omega)$ are contributions from rotational and translational diffusion of water molecules, respectively, and defined as

$$S_R(Q,\omega) = j_0^2(Qa)\,\delta(\omega) + 3j_1^2(Qa)\,L(\omega,1/3\tau_R) + 5j_2^2(Qa)\,L(\omega,1/\tau_R) \quad (3)$$

$$S_T(Q,\omega) = L(\omega,\Gamma_T) \quad (4)$$

Here, $j_l(x)$ are spherical Bessel functions. $L(\omega,\Gamma)$ is a Lorentzian function of an argument ω and a half-width at half-maximum (hwhm) Γ. a stands for radius of rotation, taken as 0.98 Å (the O−H distance of water molecule). τ_R denotes the relaxation time of rotational diffusion. The higher order terms in eq 3 are negligible in our experimental Q range. Γ_T is defined as

$$\Gamma_T = \frac{D_T Q^2}{1 + D_T Q^2 \tau_T} \quad (5)$$

where D_T is the self-diffusion coefficient and τ_T the residence time of translational diffusion. The model mentioned above is a rather strict one but contains too many parameters to be determined. We assumed that a part of monolayer water molecules are immobile in the experimental time scale and the remaining water molecules have the same dynamic property as capillary-condensed water molecules (model 1). The observed spectra of the water-filled samples were analyzed with the following scattering law:

$$S(Q,\omega) = \exp(-Q^2\langle u^2\rangle/3)[A\delta(\omega) + (1 - A)S_R(Q,\omega) \otimes S_T(Q,\omega)] + B \quad (6)$$

where A is a fraction of the elastic component.

The spectra were analyzed in a least-squares refinement procedure by using a program KIWI[13] in which the experimental data were fitted by $S(Q,\omega)$ convoluted by the resolution function of the instrument. The detail of the least-squares fitting procedure is as follows. First, eight spectra measured at 300 K in different ranges of scattering angles were fitted simultaneously by the model function. At low temperature, the line width of quasi-elastic component becomes narrower, which causes ambiguity of fitting. Then, we assumed that fraction A of elastic component for each sample does not change with temperature. Spectra at lower temperatures were fitted with imposing the A values determined from the spectra at 300 K. Examples of the least-squares fitting are shown in Figures 4 and 5.

The parameters obtained by the fitting are listed in Table 3. Values of parameters could not be determined for the data obtained at the lowest temperature (∼200 K), because their line widths became the same order as that of the resolution function. In other words, all the atoms in the samples are immobile in the experimental time scale at this temperature. Therefore, we used the data measured at temperatures above 240 K in the following discussion. We tried to fit the spectra at the temperatures 240−250 K by using a model in which the capillary-condensed water molecules move only rotationally, because the motion of the water molecules at these temperatures might be different from that at room temperature. This trial, however, failed because the fractions of elastic component obtained became negative. This implies that the translational motions of the water molecules still occur at these temperatures. In this experiment, the fraction A of elastic component is determined only by the fraction of the immobile protons, as mentioned above. The A values obtained, listed in Table 3, seem reasonable because these values correspond to the situation in which all of the protons of surface hydroxyls and a part of the protons of the monolayer water molecules are immobile. The translational self-diffusion coefficient D_T at 300 K decreases with narrowing the pore size. The mean jump lengths L were estimated from the obtained values of τ_T and D_T by using the relation[14] $L =$

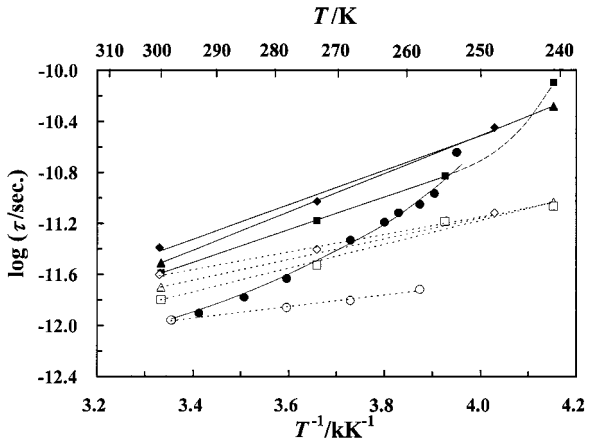

Figure 8. Arrhenius plot of the relaxation time of rotational diffusion (open symbols) and the residence time of translational diffusion (closed symbols) determined by using model 1 for the water-filled C10 (diamonds), C14 (triangles), and C18 (squares) samples. Literature values[12] for bulk water (circles) are plotted for comparison.

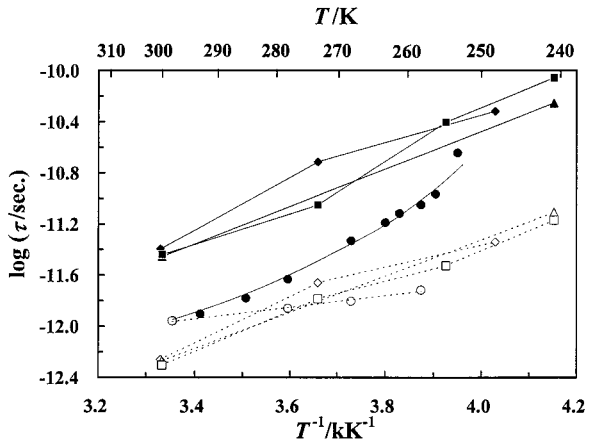

Figure 9. Arrhenius plot of the relaxation time of rotational diffusion (open symbols) and the residence time of translational diffusion (closed symbols) determined by using model 2 for the water-filled C10 (diamonds), C14 (triangles), and C18 (squares) samples. Literature values[12] for bulk water (circles) are plotted for comparison.

$(6\tau_T D_T)^{1/2}$. The L values determined in Table 3 are the same order as the molecular size of water and thus reasonable for the model employed here. It should be pointed out that the D_T values obtained below 273 K contain relatively large errors. The reason for this is that D_T is mainly determined from the spectra at small Q ranges where the line widths of spectra become narrow. Thus, the temperature dependence of D_T values is not discussed in this paper.

Figure 8 shows an Arrhenius plot of the relaxation time τ_R of rotational diffusion and the residence time τ_T of translational diffusion. For comparison, the literature values[12] for bulk water are also shown. Both τ_R and τ_T values for MCM-41 samples showed the Arrhenius type of temperature dependence, except for τ_T for the C18 sample at 241 K where the water in pores begins to freeze. The activation energies (ΔE_R and ΔE_T) of rotational and translational diffusions were determined from the gradients of the Arrhenius plot and are listed in Table 3. The temperature dependence of τ_T for bulk water is clearly a non-Arrhenius type. This is explained by the growth of the hydrogen-bond network with lowering of the temperature and may be a precursor of the singularity at −45 °C. The Arrhenius behavior of τ_T data for the present samples will be attributed to inhibition of the growth of the hydrogen-bond network in the confined water by the surface field. This result may be consistent with the fact that the singularity phenomenon was not observed in the DSC measurement for the present samples. It is another remarkable point that both τ_R and τ_T of the present samples are, on the whole, longer than those of bulk water. According to the Eyring rate theory,[15] this result corresponds to a decrease in the activation entropy or an increase of the activation energy. Unfortunately, it could not be clarified from the present data which the dominant factor is. If the former factor is dominant, it may be attributed to the limitation of path for the translation of water molecules by impermeable pore walls. Finally, there is a trend that the smaller the pore size the larger the τ_R and τ_T values. This trend was especially clear at 300 K. It can be reasonably explained by an increase in the ratio of water molecules neighboring the silica surface.

Data Analysis for the Sample Having Monolayer Water. The quality of the spectra of the sample having monolayer water is inferior to those of the water-filled samples because its water content is small. We should introduce some assumptions in the data analysis. First, we assumed that the translational diffusion of the water molecules was slow. In this case, the scattering law can be represented by the following equation:

$$S(Q,\omega) = \exp(-Q^2\langle u^2\rangle/3)[A\delta(\omega) + (1-A)S_{R,ml}(Q,\omega)] + B \quad (7)$$

where $S_{R,ml}(Q,\omega)$ is a scattering law of the monolayer water and has the same form as $S_R(Q,\omega)$ in eq 3. Next, the value of A was fixed at 0.157, which was determined from the adsorption isotherm of water. Examples of the least-squares fitting are shown in Figure 7. The parameters obtained by the fitting are listed in Table 3. From the values obtained for relaxation time of the monolayer water ($\tau_{R,ml}$), it was found that the rotational motion of monolayer water molecules is almost the same as that of the capillary-condensed water.

Additional Data Analysis for Water-Filled Samples (Model 2). We tried to perform another data analysis for water-filled samples in which the dynamics of the monolayer water was distinguished from that of capillary-condensed water. This analysis is an additional one because we used many assumptions to reduce the number of unknown parameters. The most important assumption is that the monolayer water molecules in water-filled sample have the same dynamics as those in the sample having only monolayer water. The scattering law of this model (model 2) can be written as follows;

$$S(Q,\omega) = \exp(-Q^2\langle u^2\rangle/3)[A_1\delta(\omega) + A_2 S_{R,ml}(Q,\omega) + (1-A_1-A_2)S_R(Q,\omega) \otimes S_T(Q,\omega)] + B \quad (8)$$

Actually, the monolayer molecules in water-filled sample must be less mobile than those in the sample having only monolayer water. The real system is located in the situation between model 1 and model 2. Concerning $S_{R,ml}(Q,\omega)$, only $\tau_{R,ml}$ is an unknown parameter. The $\tau_{R,ml}$ values of each sample at various temperatures were calculated from the Arrhenius-type equation

$$\tau_{R,ml} = \tau_0 \exp(\Delta E/RT) \quad (9)$$

with $\tau_0 = 0.59$ ps and $\Delta E = 3.66$ kJ mol^{-1}, which were determined by the temperature dependence of $\tau_{R,ml}$ for the C18 sample having monolayer water. The values of A_1 and A_2 were fixed to the fraction of each component estimated from the adsorption isotherm of water (see Table 2). Figure 9 shows Arrhenius plots of τ_R and τ_T determined by using model 2. The

results are scattered, but qualitatively similar to the results of model 1, except for the small values of τ_R. We could not confirm whether τ_R of capillary-condensed water is shorter than that of bulk water because the results from models 1 and 2 are contrary to each other. The other conclusions from model 1 were not affected by the results of the analysis using model 2.

Conclusions

The dynamics of water molecules confined in MCM-41 was investigated by neutron scattering, and the following results were obtained.

1. τ_T for the water-filled samples showed the Arrhenius type of temperature dependence, in contrast to a remarkable non-Arrhenius behavior of that of bulk water. This implies that the growth of the hydrogen-bond network in the confined water is hindered by the surface field.

2. τ_T of the water-filled samples was, on the whole, longer than those of bulk water. The mechanism could not be clarified from the present data. One probable answer is the limitation ofthe path for translation of water molecules by impermeable pore walls.

3. There was a trend that both τ_R and τ_T of the water-filled samples increased with narrowing of the pore size according to model 1. This can be reasonably explained by an increase in the amount of water molecules neighboring the silica surface.

4. Spectra of MCM-41 sample having monolayer water were analyzed with a model in which motions of the monolayer water molecules are only rotation. The rotational motion of monolayer water molecules is similar to that of the capillary-condensed water.

The experimental separation of rotational and translational motions is now planned by using neutron beams varying in wavelength.

Acknowledgment. This work was partly supported by Grant in Aid for Science Research No. 08454227 from the Ministry of Education, Science and Culture of Japan and by a Special Grant for Cooperative Research administered by Japan Private School Promotion Foundation. We are deeply indebted to Professor T. Kajitani of Tohoku University for his kind suggestions in experiments and discussions.

References and Notes

(1) *Water, A Comprehensive Treatise*; Franks, F., Ed.; Plenum Press: New York and London, 1982; Vol. 7.
(2) Bellissent-Funel, M.-C.; Chen, S. H.; Zanotti, J.-M. *Phys. Rev. E* **1995**, *51*, 4558.
(3) Ramsay, J. D. F.; Poinsignon, C. *Langmuir* **1987**, *3*, 320.
(4) Takamuku, T.; Yamagami, M.; Wakita, H.; Masuda, Y.; Yamaguchi, T. *J. Phys. Chem. B* **1997**, *101*, 5730.
(5) Beck, J. S.; Vartuli, J. C.; Roth, W. J.; Leonowicz, M. E.; Kresge, C. T.; Schmitt, K. D.; Chu, C. T.-U.; Olson, D. H.; Sheppard, E. W.; McCullen, S. B.; Higgins, J. B.; Schlenker, J. L. *J. Am. Chem. Soc.* **1992**, *114*, 10834.
(6) Hansen, E. W.; Stocker, M.; Schmidt, R. *J. Phys. Chem.* **1996**, *100*, 2195.
(7) Hansen, E. W.; Schmidt, R.; Stocker, M.; Akporiaye, D. *J. Phys. Chem.* **1995**, *99*, 4148.
(8) Morishige, K.; Nobuoka, K. *J. Chem. Phys.* **1997**, *107*, 6965.
(9) Kajitani, T.; Shibata, K.; Ikeda, S.; Kohgi, M.; Yoshizawa, H.; Nemoto, K.; Suzuki, K. *Physica B* **1995**, *213&214*, 872.
(10) Jackson, C. L.; McKenna, G. B. *J. Chem. Phys.* **1990**, *93*, 9002.
(11) Bee, M. *Quasielastic Neutron Scattering*; Adam Hilger: Bristol and Philadelphia, 1987.
(12) Teixeira, J.; Bellissent-Funel, M.-C.; Chen, S. H.; Dianoux, A. J. *Phys. Rev. A* **1985**, *31*, 1913.
(13) A fit program for quasi-elastic data analysis, "KIWI ver.1.01" made by Fanjat, N.
(14) Egelstaff, P. A. *An Introduction to the Liquid State*; Academic Press: London and New York, 1967.
(15) Glasstone, S.; Laidler, K. J.; Eyring, H. *The Theory of Rate Processes*; McGraw-Hill: New York, 1949.
(16) Chen, S. H. *Hydrogen-Bonded Liquids*; NATO Advanced Study Institute, Series C, 329; Dore, J. C., Teixeira, J., Eds.; Kluwer Academic: Dordrecht, 1991; p 289.